Token-Budget Distillation: Transferring Full-Token Semantics to Compressed Video Vision-Language Models

Xiaoyang Guo
Sun Yat-sen University
Guangzhou, Guangdong, China
guoxy77@mail2.sysu.edu.cn

Guoping Luo
The University of British Columbia
Vancouver, British Columbia, Canada
luoguoping2022@163.com

Jusheng Zhang
Sun Yat-sen University
Guangzhou, Guangdong, China
jushengzhang88889@gmail.com

Keze Wang*
Sun Yat-sen University
Guangzhou, Guangdong, China
kezewang@gmail.com

Wenhao Wang*
Vast Intelligence Lab
Sydney, New South Wales, Australia
wangwenhao@vastilab.com

arXiv:2608.28138v2 [cs.CV] 19 Oct 2026

Abstract

Adapting video vision-language models (VLMs) is computationally expensive because video inputs produce a large number of visual tokens, making both fine-tuning and inference costly. Although visual token compression can reduce this overhead, direct adaptation on compressed inputs often causes semantic drift and noticeable performance degradation. We present Token-Budget Distillation (TBD), a parameter-efficient fine-tuning framework for adapting video VLMs under a fixed token budget. TBD freezes the pretrained backbone, updates only LoRA adapters, and integrates FlashVID-based visual token compression into the video pathway. To preserve full-token semantics under compression, TBD employs a dual-path teacher-student design, where a full-token teacher provides stable supervision and a compressed student is optimized with task loss, answer-region KL distillation, GT-anchored margin distillation, and reliability-aware KD control. This design enables the student to recover the semantic behavior of the full-token model while remaining efficient under aggressive token reduction. We evaluate TBD on three video VLM backbones, including LLaVA-Video, LLaVA-OneVision, and Qwen3-VL-8B-Instruct, across four video understanding benchmarks. TBD consistently outperforms compression-only baselines under both moderate and aggressive compression. On LLaVA-Video at retention ratio R=10%, TBD preserves 97.0% of the Vanilla model's average accuracy; on LLaVA-OneVision at R=10%, it achieves an average score of 58.4 and matches 100.0% relative accuracy.

CCS Concepts

• **Computing methodologies** → **Computer vision**; *Machine learning*; • **Information systems** → Multimedia information systems.

Keywords

Video Vision-Language Models; Token-Budget Distillation; Token Compression; Parameter-Efficient Fine-Tuning; Video Understanding

ACM Reference Format:
Xiaoyang Guo, Guoping Luo, Jusheng Zhang, Keze Wang, and Wenhao Wang. 2026. Token-Budget Distillation: Transferring Full-Token Semantics to Compressed Video Vision-Language Models. In *Proceedings of the 34th ACM International Conference on Multimedia (MM '26), November 10–14, 2026, Rio de Janeiro, Brazil.* ACM, New York, NY, USA, 10 pages. https://doi.org/10.1145/3767308.3835088

*Corresponding authors.

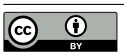
This work is licensed under a Creative Commons Attribution 4.0 International License.
MM '26, Rio de Janeiro, Brazil
© 2026 Copyright held by the owner/author(s).
ACM ISBN 979-8-4007-2213-4/2026/11
https://doi.org/10.1145/3767308.3835088

1 Introduction

Recent advances in video vision-language models (VLMs) have led to strong performance on video question answering, instruction following, and long-video understanding tasks [2, 19, 25, 28, 36, 52, 54, 56, 61]. Representative systems such as Video-ChatGPT [28], Video-LLaVA [25], LLaVA-OneVision [19], LLaVA-Video [61], and the Qwen-VL [2, 36] family demonstrate that large multimodal backbones can reason over spatiotemporal visual content when provided with rich video representations. However, adapting these models remains computationally prohibitive. Compared with static images, videos trigger a "token explosion" across frames, causing the cost of both fine-tuning and inference to scale with sequence length.

While visual token compression has emerged as a promising way to mitigate this overhead, existing methods predominantly treat compression as a post-hoc inference accelerator. Recent token pruning and merging methods show that a large fraction of visual tokens can be removed or merged with limited loss in accuracy [3, 4, 42, 45, 46, 53]. This idea has also been extended to video settings through methods such as PruneVid [15], FrameFusion [10], FastVID [33], and FlashVID [8], which reduce spatiotemporal redundancy to improve efficiency. In particular, training-free video compression methods are attractive because they can be plugged into existing video VLMs without retraining the compression module itself [8, 47, 48, 50, 51, 55]. When fine-tuning is inherently required under a strict token budget, directly applying task supervision on compressed inputs exposes a critical vulnerability: **nontrivial semantic drift**. Specifically, the indiscriminate merging or dropping of spatiotemporal tokens often dilutes fine-grained foreground actions into aggregated background noise. Consequently, the student

model's visual attention drifts from precise, discriminative actions (e.g., "Riding a bicycle") towards ambiguous, generalized conceptual representations (e.g., "Moving object"). This leads to degraded confidence and a significant loss of the full-token model's original semantic reasoning capability.

To bridge this gap, we propose **Token-Budget Distillation (TBD)**, a parameter-efficient fine-tuning framework that shifts the paradigm from simple compression-aware tuning to *teacher-guided semantics preservation*. As detailed in the dual-branch architecture in Figure 1, TBD maps the robust knowledge of a full-token teacher into a compressed student operating under a stringent token budget. TBD freezes the pretrained backbone and updates only LoRA adapters [13], integrating FlashVID-based compression into the forward pathway. To ensure stable transfer despite severe token reduction, we formulate a reliable distillation module that synergizes answer-region KL distillation [11, 49], ground-truth-anchored margin distillation, and dynamic KD warmup.

TBD goes beyond macro-level accuracy to mechanistically rehabilitate the compressed model's internal representations. Rather than treating the VLM as a black box, we counteract semantic drift through targeted constraints computed within our distillation module. Answer-region KL alignment ensures the student only mimics the teacher's most confident and relevant token distributions, filtering out noise and pulling the student's conceptual embedding back to the teacher's manifold. Simultaneously, the GT-anchored margin distillation enforces a robust confidence gap between the target response and competing tokens.

We evaluate TBD on three video VLM backbones—LLaVA-Video [61], LLaVA-OneVision [19], and Qwen3-VL-8B-Instruct [2]—across four video understanding benchmarks: MVBench [21], VideoMME [9], EgoSchema [29], and LongVideoBench [38]. TBD consistently and substantially outperforms compression-only baselines under both moderate ($R = 20\%$) and aggressive ($R = 10\%$) compression regimes. Notably, on LLaVA-Video at an aggressive $R = 10\%$ retention ratio, TBD preserves 97.0% of the Vanilla model's average accuracy; on LLaVA-OneVision at $R = 10\%$, it achieves an average score of 58.4, fully matching 100.0% relative accuracy.

Our contributions are summarized as follows:

- **Identification of Semantic Drift:** We pinpoint and formalize the semantic drift pathology caused by direct fine-tuning on compressed visual tokens, demonstrating how spatial dilution leads to cognitive ambiguity, thus reframing efficient adaptation as a semantics preservation challenge.
- **Token-Budget Distillation Framework:** We propose TBD, a compression-aware LoRA adaptation framework. As illustrated in Figure 1, by integrating answer-region KL alignment, GT-anchored margin supervision, and reliability-aware KD control, TBD safely transfers full-token semantics to a severely budgeted student.
- **Deep Mechanistic Insights & Empirical Success:** TBD achieves consistent state-of-the-art accuracy-efficiency tradeoffs across three major video VLM backbones. Beyond macro-metrics, our analyses show that TBD rectifies output distribution misalignment, reconstructs robust decision boundaries, and arrests visual attention drift.

2 Related Work

Video vision-language models. Recent video vision-language models extend large multimodal architectures from images to videos and have rapidly improved performance on video understanding tasks. Early representative efforts, including VideoChat [20], Valley [27], Video-LLaMA [44], Video-ChatGPT [28], and Video-LLaVA [25], demonstrated that large language models can be coupled with video encoders for conversational, instruction-following, and temporally aware video understanding. Subsequent works further explored long-video memory, compact visual representation, temporal grounding, and efficient transfer from image-based backbones, as in MovieChat [34], LLaMA-VID [24], VTimeLLM [14], PLLaVA [40], ST-LLM [26], Video-STaR [62], and VideoLLaMA 2 [6]. More recent models, such as LLaVA-OneVision [19], LLaVA-Video [61], Qwen2-VL [36], and Qwen3-VL [2], further strengthen video reasoning through improved architectural design and instruction-tuning data. Despite their differences in spatiotemporal modeling, long-context handling, and positional encoding, these models share the same computational bottleneck: the number of visual tokens grows rapidly with video length. This inevitably leads to quadratic complexity in self-attention mechanisms, making both fine-tuning adaptation and real-time inference increasingly expensive. This critical scaling behavior motivates the problem setting studied in our work.

Visual token compression for video VLMs. To reduce the computational burden of long visual sequences, a large body of work studies visual token reduction for multimodal models. Representative generic pruning and merging methods include ToMe [3], FastV [4], PyramidDrop [39], SparseVLM [60], LLaVA-PruMerge [31], VisPruner [59], DivPrune [1], TopV [41], VScan [43], and VisionZip [42]. Recent extensions to video VLMs further model temporal or spatiotemporal redundancy, including PruneVid [15], FrameFusion [10], FastVID [33], DyCoke [35], STTM [16], HoliTom [32], DyToK [23], and FlashVID [8]. These methods typically exploit spatial homogeneity or temporal continuity to filter out uninformative background patches or fuse visually correlated regions. However, they mainly treat compression as a plug-and-play acceleration module and focus on efficient inference. By contrast, our work does not propose a new compression operator; instead, it studies how a video VLM should be *adapted* once compression is introduced into the training pipeline, with particular emphasis on mitigating the severe semantic drift that occurs during fine-tuning.

Parameter-efficient adaptation and distillation. Parameter-efficient fine-tuning reduces adaptation cost by updating only a small subset of parameters rather than the full backbone. Representative approaches include adapters [5, 12, 57], prefix tuning [22], prompt tuning [18], LoRA [13], AdaLoRA [58], and QLoRA [7]. Knowledge distillation provides a complementary route to efficient transfer, with representative methods including the original teacher-student framework [11], DistilBERT [30], TinyBERT [17], and MiniLM [37]. Existing PEFT and distillation methods, however, do not explicitly address the mismatch introduced by token-compressed video inputs. Crucially, standard distillation paradigms assume a one-to-one token correspondence or consistent feature manifolds between teacher and student, an assumption that collapses when inputs are aggressively compressed.

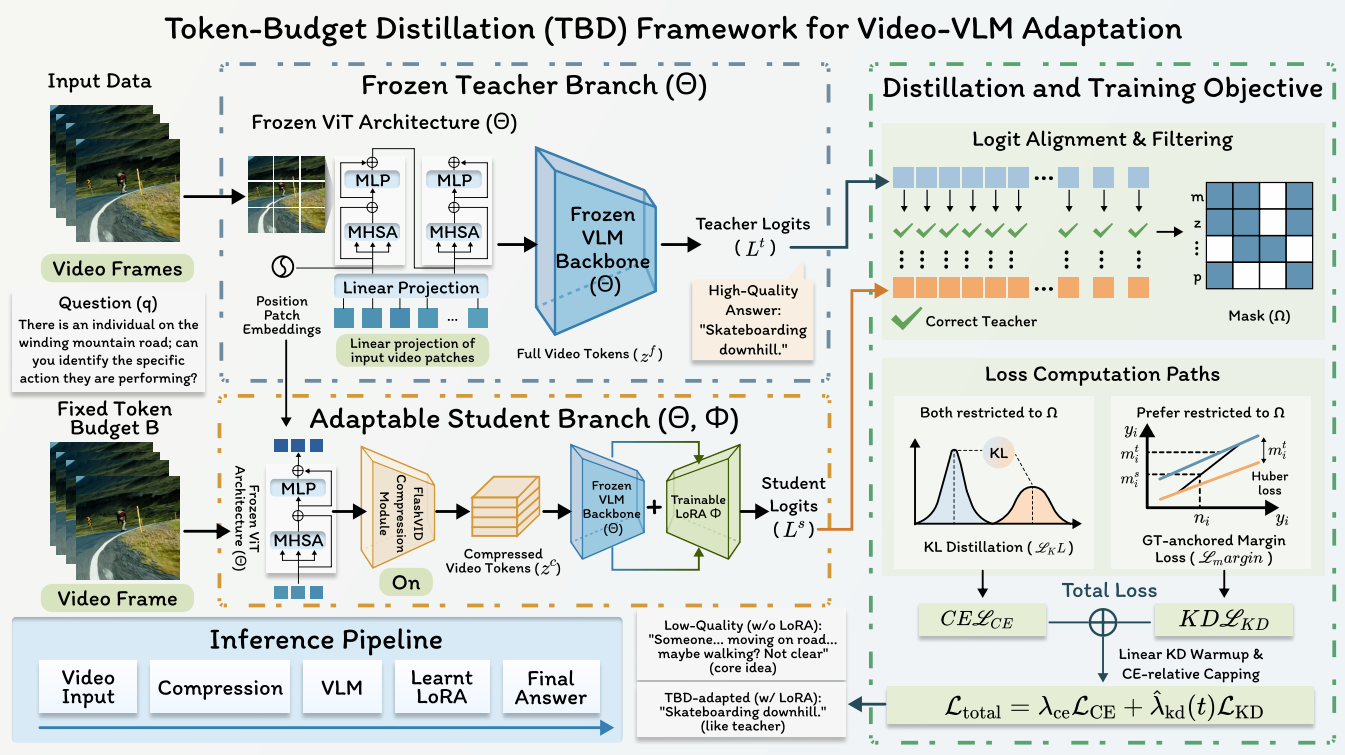

Figure 1: Overview of the Token-Budget Distillation (TBD) framework. A full-token teacher branch provides reliable guidance, while a compressed student branch with LoRA is optimized under a fixed token budget.

3 Method

3.1 Problem Setup

We study the efficient adaptation of a video vision-language model (VLM) under a strict visual token budget. Let $\mathcal{D} = \{(v, q, y)\}$ denote the training set, where v is a video, q is the textual instruction or question, and $y = (y_1, \ldots, y_T)$ is the target answer sequence. In long-video scenarios, the number of visual tokens scales linearly with the number of frames, leading to a quadratic explosion in self-attention complexity that makes both fine-tuning and inference computationally prohibitive.

To mitigate this bottleneck, we consider a token-budgeted setting where the model is constrained to consume at most B visual tokens per video sample. Given the full visual token sequence $\mathbf{z}^f = \{z_1, \ldots, z_{N_f}\}$ extracted from v, we apply a compression operator $C(\cdot; B)$ to yield a compact sequence:

$$\mathbf{z}^c = C(\mathbf{z}^f; B), \quad |\mathbf{z}^c| = N_c \le B \ll N_f, \tag{1}$$

where $\mathbf{z}^f$ and $\mathbf{z}^c$ denote the full and compressed token representations, respectively. In our implementation, C is instantiated via FlashVID-based spatiotemporal token compression along the video pathway. The fundamental challenge lies in preserving the fine-grained visual semantics critical for accurate reasoning when operating on this heavily compressed representation.

Our objective is to adapt the model to operate efficiently on $\mathbf{z}^c$ while strictly preserving the semantic reasoning capabilities of the full-token model. To achieve this, we freeze the pretrained backbone parameters Θ and optimize only a set of low-rank adaptation (LoRA) parameters Φ. Formally, the optimization target is formulated as:

$$\Phi^* = \arg\min_{\Phi} \sum_{(v,q,y)\in\mathcal{D}} \mathcal{L}\big(y; v, q, \mathbf{z}^f, \mathbf{z}^c; \Theta, \Phi\big), \tag{2}$$

where $\mathcal{L}$ elegantly combines the standard supervised objective with our proposed reliability-aware distillation constraints, as detailed in the subsequent subsections.

3.2 Token-Budget Distillation Framework

Building upon this formulation, we propose *Token-Budget Distillation* (TBD), a dual-path training framework designed to seamlessly map full-token semantics into a compressed-token student (Figure 1). For each training instance (v, q, y), TBD constructs two distinct forward pathways from the identical pretrained backbone: a *teacher* branch processing $\mathbf{z}^f$ and a *student* branch processing $\mathbf{z}^c$.

The teacher branch operates with compression disabled and LoRA adapters deactivated, effectively acting as an exact proxy for the original full-token model. Let

$$\mathbf{L}^t = f(v, q; \mathbf{z}^f, \Theta), \qquad \mathbf{L}^s = f(v, q; \mathbf{z}^c, \Theta, \Phi), \tag{3}$$

denote the next-token logit sequences for the teacher and student, respectively. The corresponding probability distributions are obtained via the softmax operator $\sigma(\cdot)$. Crucially, $\mathbf{L}^t$ is generated in a gradient-free evaluation mode, whereas $\mathbf{L}^s$ is produced by the trainable compressed branch.

This asymmetric architecture ensures that the teacher branch provides a robust, anchor-like full-token target, compelling the student to reconstruct this high-fidelity behavior from scarce visual evidence. Post-adaptation, the teacher branch is discarded, yielding a highly efficient student for inference.

Algorithm 1 Token-Budget Distillation (TBD) Optimization

Input: Training set $\mathcal{D}$, frozen VLM backbone Θ, trainable LoRA adapters Φ, compression budget B, KD hyperparameters $(\lambda_{\text{ce}}, \lambda_{\text{m}}, \lambda_{\text{kd}})$.
Output: Optimized student LoRA parameters Φ^*

for each batch $(v, q, y) \in \mathcal{D}$ **do**
  # 1. Full-Token Teacher Forward (No Gradient)
  Extract full visual token sequence $\mathbf{z}^f$ from v
  $\mathbf{L}^t \leftarrow f(v, q; \mathbf{z}^f, \Theta)$ # Compression disabled
  # 2. Compressed Student Forward (With Gradient)
  $\mathbf{z}^c \leftarrow C(\mathbf{z}^f; B)$ # FlashVID compression
  $\mathbf{L}^s \leftarrow f(v, q; \mathbf{z}^c, \Theta, \Phi)$ # LoRA enabled
  # 3. Reliability Masking & Alignment
  Identify aligned answer positions $M = \min(M_t, M_s)$
  Initialize $\Omega \leftarrow \emptyset$
  for $i = 1$ **to** M **do**
    if Teacher is correct and confident at step i **then**
      $\Omega \leftarrow \Omega \cup \{i\}$
    end if
  end for
  # 4. Objective Computation
  Compute Task Loss: $\mathcal{L}_{\text{CE}} \leftarrow \text{CrossEntropy}(\mathbf{L}^s, y)$
  Compute KL Alignment: $\mathcal{L}_{\text{KL}} \leftarrow \text{KL-Div}(\mathbf{L}^t_\Omega, \mathbf{L}^s_\Omega)$
  Compute Margin Gap: $\mathcal{L}_{\text{margin}} \leftarrow \text{Huber}(\mathbf{m}^s_\Omega, \mathbf{m}^t_\Omega)$
  Calculate Distillation Loss: $\mathcal{L}_{\text{KD}} \leftarrow \mathcal{L}_{\text{KL}} + \lambda_{\text{m}}\mathcal{L}_{\text{margin}}$
  # 5. Dynamic Weighting & Update
  Update $\hat{\lambda}_{\text{kd}}(t)$ via warmup and CE-relative capping
  $\mathcal{L} \leftarrow \lambda_{\text{ce}}\mathcal{L}_{\text{CE}} + \hat{\lambda}_{\text{kd}}(t)\mathcal{L}_{\text{KD}}$
  $\Phi \leftarrow \Phi - \eta\nabla_\Phi \mathcal{L}$
end for

3.3 Compression-Aware LoRA Adaptation

The student branch harmonizes visual token compression with parameter-efficient fine-tuning (PEFT). Specifically, FlashVID compresses the spatiotemporal token sequence $\mathbf{z}^f$ into $\mathbf{z}^c$ before it enters the core language model. We integrate FlashVID as a dynamic runtime module whose state (on/off) dictates whether the backbone acts as the student or teacher.

To enable adaptation under this compression, we freeze the backbone Θ and inject LoRA parameters Φ. For any adaptable linear transformation with pretrained weights W_0, the updated weight is parameterized as:

$$W = W_0 + \Delta W, \qquad \Delta W = B_W A_W, \tag{4}$$

where $A_W \in \mathbb{R}^{r\times d}$ and $B_W \in \mathbb{R}^{d'\times r}$ are trainable low-rank matrices ($r \ll \min(d, d')$). Compression and adaptation thus serve complementary purposes: FlashVID tackles the efficiency bottleneck by slashing the sequence length, while LoRA neutralizes the ensuing semantic drift via targeted residual updates.

Notably, the token selection and merging mechanisms within FlashVID remain entirely training-free. Gradients only flow through the compressed representations to update the LoRA adapters, allowing TBD to dedicate its entire learning capacity to representation rehabilitation rather than optimizing the compression logic itself.

3.4 Reliable Distillation Under Token Compression

Compression-aware task tuning alone is insufficient to prevent semantic drift. We therefore distill the student's output toward the teacher's full-token predictions. However, token compression fundamentally alters the model's predictive certainty; thus, uniform distillation across all tokens introduces harmful noise. To combat this, TBD introduces *reliable answer-region distillation*, explicitly isolating high-quality transfer signals.

Following standard causal language modeling, we shift the logits and identify valid answer positions. Let $\mathbf{l}^t_i$ and $\mathbf{l}^s_i$ represent the aligned teacher and student logits at position i. Given valid answer lengths M_t and M_s, we define the alignment horizon as $M = \min(M_t, M_s)$.

Within this aligned region, we compute a token-level KL divergence:

$$\mathcal{L}_{\text{KL}} = \frac{1}{|\Omega|}\sum_{i\in\Omega} \text{KL}\Big(\sigma(\mathbf{l}^t_i/\tau) \parallel \sigma(\mathbf{l}^s_i/\tau)\Big)\tau^2, \tag{5}$$

where τ is the temperature. The critical innovation here is the construction of the reliability mask Ω. We populate Ω exclusively with positions where the teacher is both *correct* (highest probability assigned to the ground-truth) and *confident* (probability exceeds a predefined threshold).

To strictly prevent margin collapse—a common symptom of semantic drift where the model struggles to differentiate between the correct concept and related background noise—we introduce *GT-anchored margin distillation*. For each $i \in \Omega$, let y_i be the ground-truth token and n_i be the hardest negative token (the highest-scoring incorrect token per the teacher). We explicitly formalize their margins:

$$m^t_i = l^t_{i,y_i} - l^t_{i,n_i}, \qquad m^s_i = l^s_{i,y_i} - l^s_{i,n_i}, \tag{6}$$

and penalize deviations using a robust Huber loss:

$$\mathcal{L}_{\text{margin}} = \frac{1}{|\Omega|}\sum_{i\in\Omega} \text{Huber}(m^s_i, m^t_i). \tag{7}$$

This ensures the compressed student mimics not just the softened distribution, but the teacher's decisive boundary gaps.

3.5 Overall Objective and Optimization

The complete optimization objective balances standard autoregressive training with our reliability-aware distillation. The primary task loss ensures fidelity to the downstream instruction:

$$\mathcal{L}_{\text{CE}} = -\frac{1}{|\mathcal{A}|}\sum_{i\in\mathcal{A}} \log \sigma(\mathbf{l}^s_i)_{y_i}, \tag{8}$$

where $\mathcal{A}$ spans all valid student answer positions.

The distillation objective aggregates the KL and margin terms:

$$\mathcal{L}_{\mathrm{KD}} = \mathcal{L}_{\mathrm{KL}} + \lambda_{\mathrm{m}} \mathcal{L}_{\mathrm{margin}}. \tag{9}$$

The final training loss is dynamically scaled:

$$\mathcal{L} = \lambda_{\mathrm{ce}} \mathcal{L}_{\mathrm{CE}} + \hat{\lambda}_{\mathrm{kd}}(t)\, \mathcal{L}_{\mathrm{KD}}. \tag{10}$$

To prevent early-stage over-regularization, $\hat{\lambda}_{\mathrm{kd}}(t)$ incorporates a linear warmup schedule and is strictly capped relative to the magnitude of $\mathcal{L}_{\mathrm{CE}}$. The complete training pipeline is summarized in Algorithm 1.

4 Experiments

4.1 Experimental Setup

Training Data and Details. We train our models strictly on the comprehensive video instruction-tuning dataset LLaVA-Video-178K [61]. This dataset is specifically chosen for its high-quality, diverse spatiotemporal annotations, ensuring that the teacher model's semantic guidance during our distillation process is rooted in complex, multi-turn reasoning rather than superficial visual matching. By utilizing a rich instruction-following corpus, we guarantee that the adapted student model learns to align compressed visual tokens with complex linguistic queries.

Evaluation Benchmarks. To rigorously assess the generalizability and robustness of TBD, we evaluate on four distinct and highly challenging video understanding benchmarks. Specifically, **VideoMME** [9] provides a comprehensive evaluation across short, medium, and long videos, testing the model's versatility; **EgoSchema** [29] challenges the model with extremely long-term, goal-oriented reasoning in egocentric videos; **LongVideoBench** [38] focuses on extended contextual memory and understanding; and **MVBench** [21] probes fine-grained spatiotemporal dynamics and micro-action recognition. By covering both macro-level narrative comprehension and micro-level action details, this evaluation suite ensures that any semantic drift, temporal hallucination, or boundary collapse caused by token compression is thoroughly exposed and quantified. Following standard protocols, we report benchmark-specific accuracy metrics and additionally summarize the average performance across all tasks to reflect the overarching accuracy-efficiency trade-off under strictly constrained token budgets.

Model Backbones. We instantiate and evaluate TBD across three highly representative, state-of-the-art video VLM backbones: LLaVA-Video [61], LLaVA-OneVision [19], and Qwen3-VL-8B-Instruct [2]. These backbones span different architectural paradigms, spatial-temporal pooling strategies, and parameter scales. Evaluating across this diverse set allows us to demonstrate the universal applicability and plug-and-play nature of our distillation framework, proving that TBD's effectiveness is not strictly tied to a specific visual encoder or LLM family.

Baselines and Compression Regimes. In the main results, we compare TBD against the original uncompressed model (Vanilla, serving as the theoretical upper bound) and a suite of representative token reduction baselines. These baselines encompass both spatial-only token dropping/merging (FastV [4], VisionZip [42]) and advanced spatiotemporal reduction techniques (FastVID [33], FlashVID [8]), representing the current landscape of training-free visual compression. For a strictly fair comparison, all compressed variants—whether training-free or adapted—are evaluated under identical visual token retention ratios. We report results at $R = 20\%$ to examine performance under a moderate efficiency bottleneck, and at a highly aggressive $R = 10\%$ regime to explicitly stress-test the model's ability to preserve cognitive reasoning when 90% of the visual evidence is permanently discarded.

4.2 Main Results

Table 1 summarizes the main results. TBD consistently improves the accuracy-efficiency trade-off of compressed video VLMs across three backbones and different compression regimes. Compared with compression-only baselines, TBD achieves the strongest or near-strongest performance on most benchmarks while operating under the same token budget. This trend indicates that the proposed distillation-based adaptation is effective at recovering the semantic information lost during token compression, especially when the retention ratio becomes more aggressive.

On LLaVA-Video, TBD achieves the best average score among compressed variants at both $R = 20\%$ and $R = 10\%$. At $R = 20\%$, it reaches an average score of 59.7, outperforming FlashVID (59.3), FastVID (58.7), VisionZip (59.0), and FastV (56.9), while retaining 98.4% of the Vanilla model's average accuracy. At the more aggressive $R = 10\%$ setting, TBD further shows clear robustness, obtaining an average score of 58.9 and preserving 97.0% of the Vanilla accuracy, again surpassing all compared compressed baselines. We also observe consistent gains on the overall VideoMME score, indicating that TBD remains effective across short, medium, and long video subsets. Similar trends hold for LLaVA-OneVision. At $R = 20\%$, TBD achieves the highest average score among compressed methods (59.0), slightly surpassing FlashVID (58.7) and even marginally exceeding the Vanilla model in relative accuracy. At $R = 10\%$, TBD remains the strongest compressed variant with an average score of 58.4, improving over FlashVID (57.9), FastVID (57.1), VisionZip (54.0), and FastV (53.6), while matching the Vanilla model in relative average accuracy. We further evaluate TBD on Qwen3-VL-8B-Instruct. Compared with FlashVID, TBD consistently improves performance at both retention ratios. At $R = 20\%$, the average score increases from 60.9 to 61.6, with gains on all four benchmarks. At the more aggressive $R = 10\%$ setting, TBD improves the average score from 58.8 to 59.4 and raises the relative accuracy from 91.3% to 92.2%. These results show that the benefit of TBD is not limited to the LLaVA family, but also generalizes to a stronger and architecturally different video VLM backbone.

Overall, these results confirm that TBD is effective across different video VLM backbones and retains its advantage under both moderate and aggressive token compression.

4.3 Ablation Study

We conduct ablation experiments on LLaVA-Video under the more challenging retention ratio $R = 10\%$ to quantify the contribution of each component in TBD. As shown in Table 2, the LoRA-only Student baseline achieves an average score of 58.3, indicating that parameter-efficient adaptation alone can partially compensate for compression, but still leaves a clear gap to the full method.

Table 1: Main results on four video understanding benchmarks under different token retention ratios. We compare TBD with the uncompressed Vanilla model and representative token reduction baselines on three backbones: LLaVA-Video, LLaVA-OneVision, and Qwen3-VL-8B-Instruct. "Avg. Score" denotes the average performance across benchmarks, and "Rel. Acc (%)" reports the average score normalized by the corresponding Vanilla model.

Method	Retention Ratio R	VideoMME				EgoSchema		LongVideo Bench	MVBench	Avg.	
		Short	Medium	Long	Overall	Subset	Total			Score	Rel. Acc (%)
LLaVA-Video											
Vanilla	100%	77.0	62.1	53.3	64.2	59.4	57.3	59.5	61.9	60.7	100.0
FastV	20%	69.3	58.3	49.9	59.2	54.8	54.1	56.0	58.4	56.9	93.7
VisionZip	20%	72.3	59.6	**53.3**	61.7	**59.0**	56.4	58.0	59.8	59.0	97.2
FastVID	20%	**74.6**	60.8	52.3	62.6	57.0	55.0	57.1	60.2	58.7	96.7
FlashVID	20%	74.1	60.0	52.3	62.2	58.4	56.4	58.7	59.8	59.3	97.7
TBD (ours)	20%	74.0	**61.0**	53.1	**62.7**	58.5	**56.6**	**59.2**	**60.3**	**59.7**	**98.4**
FastV	10%	64.3	53.8	49.2	55.8	50.6	51.1	53.6	56.2	54.2	89.3
VisionZip	10%	69.4	57.9	51.2	59.5	54.4	53.9	54.5	58.5	56.6	93.2
FastVID	10%	71.8	57.3	50.2	59.8	54.8	52.4	56.9	59.3	57.1	94.1
FlashVID	10%	72.2	59.1	51.2	60.9	57.2	54.9	57.7	59.3	58.2	95.9
TBD (ours)	10%	**73.6**	**60.4**	**52.6**	**62.2**	**57.4**	**55.2**	**58.1**	**60.0**	**58.9**	**97.0**
LLaVA-OneVision											
Vanilla	100%	69.9	56.7	48.9	58.5	62.2	60.3	56.6	58.3	58.4	100.0
FastV	20%	66.3	53.9	46.9	55.7	60.6	57.6	56.0	56.0	56.3	96.4
VisionZip	20%	68.6	**57.0**	48.3	58.0	62.0	60.0	55.4	57.6	57.7	98.8
FastVID	20%	69.9	56.3	47.4	57.9	61.2	59.5	55.9	58.1	57.9	99.1
FlashVID	20%	70.1	55.4	48.9	58.2	**63.0**	60.1	58.5	58.2	58.7	100.5
TBD (ours)	20%	**71.3**	56.8	**49.1**	**59.1**	62.9	**60.1**	**58.6**	**58.3**	**59.0**	**101.0**
FastV	10%	60.9	52.2	44.9	52.7	59.0	56.0	52.4	53.4	53.6	91.8
VisionZip	10%	60.3	52.9	46.7	53.3	61.6	58.5	49.4	54.8	54.0	92.5
FastVID	10%	68.1	55.7	47.8	57.2	58.8	58.7	55.7	57.0	57.1	97.8
FlashVID	10%	67.3	57.1	49.0	57.8	62.4	60.0	56.5	57.4	57.9	99.1
TBD (ours)	10%	**68.5**	**58.4**	**50.2**	**59.0**	**62.4**	**60.1**	**56.9**	**57.7**	**58.4**	**100.0**
Qwen3-VL-8B-Instruct											
Vanilla	100%	74.6	60.8	56.3	63.9	66.2	68.3	59.2	66.3	64.4	100.0
FastVID	20%	66.9	54.1	51.8	57.6	62.2	62.0	56.7	63.3	59.9	93.0
FlashVID	20%	68.3	55.3	52.1	58.6	64.4	63.2	57.2	64.6	60.9	94.6
TBD (ours)	20%	**69.2**	**56.4**	**53.0**	**59.5**	**65.0**	**63.8**	**57.9**	**65.1**	**61.6**	**95.7**
FastVID	10%	64.6	54.5	49.3	56.1	61.8	61.4	54.6	58.9	57.8	89.8
FlashVID	10%	66.1	55.3	49.8	57.1	63.0	62.2	55.2	60.5	58.8	91.3
TBD (ours)	10%	**67.3**	**56.3**	**50.6**	**58.1**	**63.5**	**62.6**	**55.8**	**61.0**	**59.4**	**92.2**

Adding answer-region KL distillation improves the average score from 58.3 to 58.6, showing that aligning the compressed student with the full-token teacher at the output-distribution level is already beneficial. When we further incorporate GT-anchored margin distillation, the score increases to 58.8, suggesting that explicitly preserving the teacher's local decision boundary provides additional gains beyond distribution matching alone.

Finally, enabling the full set of reliability filtering and CE-relative KD capping yields the best result, reaching 58.9 average score and 97.0% relative accuracy. Although the improvement over the previous variant is smaller, it is consistent with the role of these mechanisms: they primarily stabilize training and suppress noisy distillation signals, thereby making the overall optimization more reliable. Overall, the ablation study confirms that the gains of TBD come

Table 2: Ablation study on LLaVA-Video at retention ratio $R = 10\%$. "Rel. Acc (%)" is normalized by the corresponding Vanilla model in Table 1.

Variant	LoRA	Answer-region KL	GT-anchored Margin	Filtering & KD Cap	Score	Rel. Acc (%)
LoRA-only Student	✓	✗	✗	✗	58.3	96.0
+ Answer-region KL	✓	✓	✗	✗	58.6	96.5
+ GT-anchored Margin	✓	✓	✓	✗	58.8	96.9
Full TBD	✓	✓	✓	✓	58.9	97.0

Table 3: Effect of different compression modules within TBD on LLaVA-Video at retention ratio $R = 10\%$. FlashVID is the default compression module used in TBD unless otherwise specified. "Rel. Acc (%)" is normalized by the corresponding Vanilla model in Table 1.

Variant	Score	Rel. Acc (%)
TBD+FastV	55.0	90.6
TBD+VisionZip	57.1	94.1
TBD+FastVID	57.7	95.1
TBD (FlashVID)	**58.9**	**97.0**

from the complementary effects of answer-region distribution alignment, margin-based boundary preservation, and reliability-aware KD control.

4.4 Effect of Compression Modules

We further examine the sensitivity of TBD to the choice of compression module by replacing FlashVID with three alternative token compression methods, namely FastVID, VisionZip, and FastV, while keeping the same TBD training objective. All comparisons are conducted on LLaVA-Video at retention ratio $R = 10\%$.

As shown in Table 3, TBD remains effective across different compression front-ends, but the choice of compression module still has a clear impact on the final performance. Among the four variants, TBD (FlashVID) achieves the best result, reaching an average score of 58.9 and 97.0% relative accuracy, followed by TBD+FastVID (57.7, 95.1%), TBD+VisionZip (57.1, 94.1%), and TBD+FastV (55.0, 90.6%). This trend is consistent with the relative strength of these compression methods in the main results.

These results suggest that TBD is not tied to a specific compression mechanism and can be combined with different token reduction strategies. At the same time, the performance gap across compression modules indicates that reliable distillation does not fully remove the influence of compression quality: a stronger compression front-end still provides a better basis for preserving full-token semantics under the same token budget.

4.5 Logit Distribution Alignment Analysis

To further examine whether TBD improves output-level alignment with the full-token teacher, we analyze next-token logits on VideoMME. Specifically, we randomly sample 100 evaluation instances and compare three models under the same setting: the full-token Teacher, a compression-only baseline, and the distilled student trained with TBD. All compressed-model analyses are conducted on LLaVA-Video with retention ratio $R = 10\%$.

For each sample, we extract the next-token logits, keep only the four answer-choice tokens $\{A, B, C, D\}$, normalize them with a softmax over the four candidates, and compute the per-sample KL divergence from the teacher distribution to each compressed model. This yields $\mathrm{KL}(P_T \| P_{\text{baseline}})$ and $\mathrm{KL}(P_T \| P_{\text{distilled}})$ for every sample. Figure 2 visualizes the resulting alignment behavior. In the left panel, each point corresponds to one VideoMME sample, plotted by its KL divergence to the teacher for the compression-only baseline and the distilled student, respectively. Points below the diagonal indicate cases where the distilled student is closer to the teacher. We observe that this occurs for 77 out of 100 samples, whereas the compression-only baseline is closer on only 23 samples. The right panel shows the corresponding KL distributions, where the mean KL divergence is reduced from 0.2310 for the compression-only baseline to 0.1172 for the distilled student. These results provide

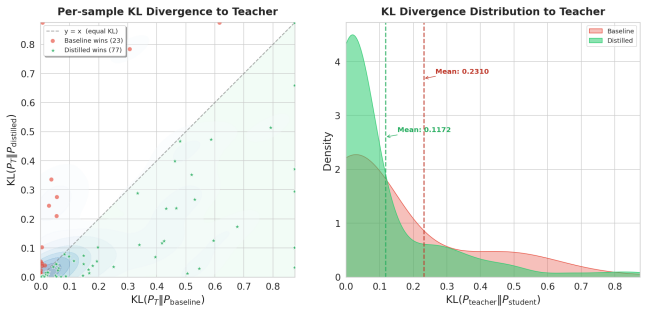

Figure 2: Logit distribution alignment on 100 randomly sampled VideoMME instances for LLaVA-Video at $R = 10\%$. Left: per-sample comparison of $\mathrm{KL}(P_T \| P_{\text{baseline}})$ and $\mathrm{KL}(P_T \| P_{\text{distilled}})$ on normalized A/B/C/D choice probabilities. Right: kernel density estimates of the KL distributions, where the distilled student shows a substantially smaller mean KL divergence to the teacher.

direct evidence for the effect of answer-region distillation. Beyond improving benchmark accuracy, TBD makes the distilled student substantially closer to the full-token teacher in the answer-choice probability space. This observation is consistent with the gains in Table 1 and supports our claim that the proposed distillation framework recovers teacher semantics under a strict token budget.

4.6 Decision Boundary Analysis

We next evaluate if GT-anchored margin distillation improves the decision boundary. We sample 200 VideoMME instances and compute the margin $\Delta = L_{gt} - L_{max_wrong}$, where L_{gt} is the ground-truth logit and L_{max_wrong} is the highest incorrect logit. A positive margin indicates confident correct predictions, while a negative one implies an incorrect preference. Figure 3 compares the compression-only baseline and our distilled student (LLaVA-Video, $R = 10\%$). The distilled student's distribution explicitly shifts rightward (left panel), reflecting a stronger preference for the correct answer. Quantitatively (right panel), the mean margin increases from 2.2325 to 2.7832, and the negative-margin ratio drops from 0.3150 to 0.2400. This confirms the distilled student better separates the correct answer from the hardest distractor and makes fewer ranking errors.

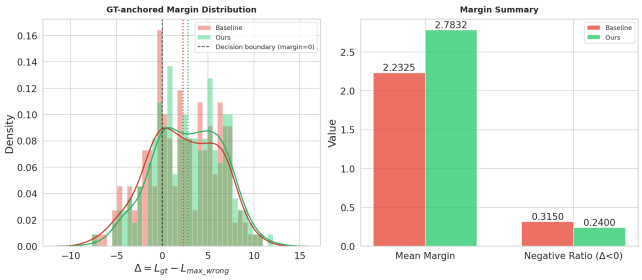

Figure 3: Decision boundary analysis on 200 randomly sampled VideoMME instances for LLaVA-Video at $R = 10\%$. Left: histogram and density of the GT-anchored margin $\Delta = L_{gt} - L_{max_wrong}$ for the compression-only baseline and the distilled student. Right: summary statistics showing that the distilled student achieves a larger mean margin and a lower negative-margin ratio.

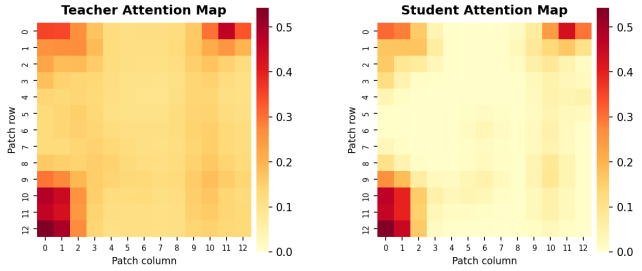

Figure 4: Attention drift visualization on a randomly selected VideoMME example for LLaVA-Video at retention ratio $R = 10\%$. We compare the teacher and distilled student attention maps on the same frame.

Consistent with Section 3.4, while KL distillation aligns overall distributions, the margin term explicitly sharpens local decision boundaries. This mechanistically explains why the full TBD objective outperforms weaker variants in Table 2.

4.7 Attention Drift Analysis

To mechanistically understand how token compression impacts the model's internal reasoning, and to qualitatively verify that TBD successfully arrests semantic drift, we conduct an in-depth visual attention analysis. In standard video VLMs, the indiscriminate removal of spatiotemporal tokens often destroys fine-grained spatial granularity. Consequently, the self-attention mechanism becomes disoriented, leading to a phenomenon where the model's visual focus drifts away from critical foreground actions and disperses into irrelevant background noise or generalized textures. To examine whether our method mitigates this pathology, we visualize and compare the spatial attention maps of the full-token Teacher and the TBD-adapted Student. We extract these maps using the LLaVA-Video backbone evaluated on the VideoMME benchmark under a highly aggressive retention ratio of $R = 10\%$. We randomly sample a representative video instance and select a keyframe to visualize the spatial attention distribution allocated to the visual tokens when generating the correct target answer. As vividly illustrated in Figure 4, the full-token Teacher acts as a reliable oracle, exhibiting a sharp, highly localized attention pattern that accurately fixates on the task-relevant foreground entities (e.g., the core action or specific object required to answer the query). Remarkably, despite operating on an aggressively truncated visual sequence where 90% of the original tokens have been discarded, the TBD-adapted student's attention map remains highly consistent with that of the teacher. Rather than collapsing into a diffuse or shifted attention distribution—a typical symptom of naive compression—the TBD student successfully allocates its severely limited token budget to the exact same salient regions identified by the teacher. This visualization yields a crucial insight: TBD does not merely act as a superficial output-level regularizer that forces logit matching. Instead, the combination of answer-region KL alignment and GT-anchored margin distillation fundamentally rehabilitates the internal multimodal routing of the network. By forcing the compressed student to reproduce the teacher's confident decision boundaries, TBD implicitly guides the student's attention heads to focus on the correct visual evidence, ensuring high efficiency without sacrificing interpretability and visual grounding.

4.8 Discussion

TBD reframes token-compressed adaptation as teacher-guided semantics recovery rather than plain task fitting, and its advantage grows as compression becomes more aggressive. The ablations confirm that the proposed mechanisms are complementary: answer-region KL distillation aligns output distributions, GT-anchored margin distillation preserves discrimination, and reliability-aware filtering stabilizes noisy signals, while the compression-module study shows TBD generalizes across front-ends, with its upper bound set by front-end quality. Mechanistically, these effects appear at multiple levels: the student matches the teacher's answer-space distribution (Figure 2), sharpens decision boundaries around the ground truth (Figure 3), and retains faithful visual focus (Figure 4), which together explain the robust gains.

5 Conclusion and Limitations

We presented *Token-Budget Distillation* (TBD), a parameter-efficient framework for adapting video VLMs under strict token budgets. By synergizing token compression, LoRA, and reliable distillation, TBD enables compressed students to recover full-token semantic behavior. Extensive experiments across multiple benchmarks and three representative backbones demonstrate that TBD consistently improves the accuracy-efficiency trade-off over compression-only baselines, especially under aggressive compression. Ultimately, our findings suggest that effective adaptation under token compression is not solely an efficiency challenge, but a semantics preservation problem. As for limitations, despite its efficacy at inference, TBD requires executing a full-token teacher during the adaptation phase, which maintains high training-time memory demands. Additionally, the student's performance upper bound is inherently constrained by the irreversible information loss of the chosen training-free compression module. We hope TBD provides a robust foundation for future research into fully memory-efficient and end-to-end compressed video VLMs.

Acknowledgments

This work was supported in part by the National Natural Science Foundation of China (NSFC) under Grant 62276283, in part by the China Meteorological Administration's Science and Technology Project under Grant CMAJBGS202517, in part by Guangdong-Hong Kong-Macao Greater Bay Area Meteorological Technology Collaborative Research Project under Grant GHMA2024Z04, in part by Fundamental Research Funds for the Central Universities, Sun Yat-sen University under Grant 23hytd006 and 23hytd006-2, and in part by Guangdong Provincial High-Level Young Talent Program under Grant RL2024-151-2-11.

References

[1] Saeed Ranjbar Alvar, Gursimran Singh, Mohammad Akbari, and Yong Zhang. 2025. Divprune: Diversity-based visual token pruning for large multimodal models. In *Proceedings of the Computer Vision and Pattern Recognition Conference*. 9392–9401.

[2] Shuai Bai, Yuxuan Cai, Ruizhe Chen, Keqin Chen, Xionghui Chen, Zesen Cheng, Lianghao Deng, Wei Ding, Chang Gao, Chunjiang Ge, et al. 2025. Qwen3-vl technical report. *arXiv preprint arXiv:2511.21631* (2025).

[3] Daniel Bolya, Cheng-Yang Fu, Xiaoliang Dai, Peizhao Zhang, Christoph Feichtenhofer, and Judy Hoffman. 2022. Token merging: Your vit but faster. *arXiv preprint arXiv:2210.09461* (2022).

[4] Liang Chen, Haozhe Zhao, Tianyu Liu, Shuai Bai, Junyang Lin, Chang Zhou, and Baobao Chang. 2024. An image is worth 1/2 tokens after layer 2: Plug-and-play inference acceleration for large vision-language models. In *European Conference on Computer Vision*. Springer, 19–35.

[5] Zheng Chen, Kai Liu, Jingkai Wang, Xianglong Yan, Jianze Li, Ziqing Zhang, Jue Gong, Jiatong Li, Lei Sun, Xiaoyang Liu, Radu Timofte, Yulun Zhang, Jihye Park, Yoonjin Im, Hyungju Chun, Hyunhee Park, MinKyu Park, Zheng Xie, Xiangyu Kong, Weijun Yuan, Zhan Li, Qiurong Song, Luen Zhu, Fengkai Zhang, Xinzhe Zhu, Junyang Chen, Congyu Wang, Yixin Yang, Zhaorun Zhou, Jiangxin Dong, Jinshan Pan, Shengwei Wang, Jiajie Ou, Baiang Li, Sizhuo Ma, Qiang Gao, Jusheng Zhang, Jian Wang, Keze Wang, Yijiao Liu, Yingsi Chen, Hui Li, Yu Wang, Congchao Zhu, Saeed Ahmad, Ik Hyun Lee, Jun Young Park, Ji Hwan Yoon, Kainan Yan, Zian Wang, Weibo Wang, Shihao Zou, Chao Dong, Wei Zhou, Linfeng Li, Jaeseong Lee, Jaeho Chae, Jinwoo Kim, Seonjoo Kim, Yucong Hong, Zhenming Yan, Junye Chen, Ruize Han, Song Wang, Yuxuan Jiang, Chengxi Zeng, Tianhao Peng, Fan Zhang, David Bull, Tongyao Mu, Qiong Cao, Yifan Wang, Youwei Pan, Leilei Cao, Xiaoping Peng, Wei Deng, Yifei Chen, Wenbo Xiong, Xian Hu, Yuxin Zhang, Xiaoyun Cheng, Yang Ji, Zonghao Chen, Zhihao Xue, Junqin Hu, Nihal Kumar, Snehal Singh Tomar, Klaus Mueller, Surya Vashisth, Prateek Shaily, Jayant Kumar, Hardik Sharma, Ashish Negi, Sachin Chaudhary, Akshay Dudhane, Praful Hambarde, Amit Shukla, Shijun Shi, Jiangning Zhang, Yong Liu, Kai Hu, Jing Xu, Xianfang Zeng, Amitesh M, Hariharan S, Chia-Ming Lee, Yu-Fan Lin, Chih-Chung Hsu, Nishalini K, Sreenath K A, Bilel Benjdira, Anas M. Ali, Wadii Boulila, Shuling Zheng, Zhiheng Fu, Feng Zhang, Zhanglu Chen, Boyang Yao, Nikhil Pathak, Aagam Jain, Milan Kumar, Kishor Upla, Vivek Chavda, Sarang N S, Raghavendra Ramachandra, Zhipeng Zhang, Qi Wang, Shiyu Wang, Jiachen Tu, Guoyi Xu, Yaoxin Jiang, Jiajia Liu, Yaokun Shi, Yuqi Li, Chuanguang Yang, Weilun Feng, Zhuzhi Hong, Hao Wu, Junming Liu, Yingli Tian, Amish Bhushan Kulkarni, Tejas R R Shet, Saakshi M Vernekar, Nikhil Akalwadi, Kaushik Mallibhat, Ramesh Ashok Tabib, Uma Mudenagudi, Yuwen Pan, Tianrun Chen, Deyi Ji, Qi Zhu, Lanyun Zhu, and Heyan Zhangyi. 2026. The Fourth Challenge on Image Super-Resolution (x4) at NTIRE 2026: Benchmark Results and Method Overview. In *Proceedings of the IEEE/CVF Conference on Computer Vision and Pattern Recognition (CVPR) Workshops*. 1697–1709.

[6] Zesen Cheng, Sicong Leng, Hang Zhang, Yifei Xin, Xin Li, Guanzheng Chen, Yongxin Zhu, Wenqi Zhang, Ziyang Luo, Deli Zhao, et al. 2024. Videollama 2: Advancing spatial-temporal modeling and audio understanding in video-llms. *arXiv preprint arXiv:2406.07476* (2024).

[7] Tim Dettmers, Artidoro Pagnoni, Ari Holtzman, and Luke Zettlemoyer. 2023. Qlora: Efficient finetuning of quantized llms. *Advances in neural information processing systems* 36 (2023), 10088–10115.

[8] Ziyang Fan, Keyu Chen, Ruilong Xing, Yulin Li, Li Jiang, and Zhuotao Tian. 2026. FlashVID: Efficient Video Large Language Models via Training-free Tree-based Spatiotemporal Token Merging. *arXiv preprint arXiv:2602.08024* (2026).

[9] Chaoyou Fu, Yuhan Dai, Yongdong Luo, Lei Li, Shuhuai Ren, Renrui Zhang, Zihan Wang, Chenyu Zhou, Yunhang Shen, Mengdan Zhang, et al. 2025. Video-mme: The first-ever comprehensive evaluation benchmark of multi-modal llms in video analysis. In *Proceedings of the IEEE/CVF conference on computer vision and pattern recognition*. 24108–24118.

[10] Tianyu Fu, Tengxuan Liu, Qinghao Han, Guohao Dai, Shengen Yan, Huazhong Yang, Xuefei Ning, and Yu Wang. 2024. FrameFusion: Combining Similarity and Importance for Video Token Reduction on Large Vision Language Models. *arXiv preprint arXiv:2501.01986* (2024).

[11] Geoffrey Hinton, Oriol Vinyals, and Jeff Dean. 2015. Distilling the knowledge in a neural network. *arXiv preprint arXiv:1503.02531* (2015).

[12] Neil Houlsby, Andrei Giurgiu, Stanislaw Jastrzebski, Bruna Morrone, Quentin De Laroussilhe, Andrea Gesmundo, Mona Attariyan, and Sylvain Gelly. 2019. Parameter-efficient transfer learning for NLP. In *International conference on machine learning*. PMLR, 2790–2799.

[13] Edward J Hu, Yelong Shen, Phillip Wallis, Zeyuan Allen-Zhu, Yuanzhi Li, Shean Wang, Lu Wang, and Weizhu Chen. 2022. LoRA: Low-Rank Adaptation of Large Language Models. In *International Conference on Learning Representations*.

[14] Bin Huang, Xin Wang, Hong Chen, Zihan Song, and Wenwu Zhu. 2024. Vtimellm: Empower llm to grasp video moments. In *Proceedings of the IEEE/CVF Conference on Computer Vision and Pattern Recognition*. 14271–14280.

[15] Xiaohu Huang, Hao Zhou, and Kai Han. 2025. Prunevid: Visual token pruning for efficient video large language models. In *Findings of the Association for Computational Linguistics: ACL 2025*. 19959–19973.

[16] Jeongseok Hyun, Sukjun Hwang, Su Ho Han, Taeoh Kim, Inwoong Lee, Dongyoon Wee, Joon-Young Lee, Seon Joo Kim, and Minho Shim. 2025. Multi-granular spatio-temporal token merging for training-free acceleration of video llms. In *Proceedings of the IEEE/CVF International Conference on Computer Vision*. 23990–24000.

[17] Xiaoqi Jiao, Yichun Yin, Lifeng Shang, Xin Jiang, Xiao Chen, Linlin Li, Fang Wang, and Qun Liu. 2020. Tinybert: Distilling bert for natural language understanding. In *Findings of the association for computational linguistics: EMNLP 2020*. 4163–4174.

[18] Brian Lester, Rami Al-Rfou, and Noah Constant. 2021. The power of scale for parameter-efficient prompt tuning. In *Proceedings of the 2021 conference on empirical methods in natural language processing*. 3045–3059.

[19] Bo Li, Yuanhan Zhang, Dong Guo, Renrui Zhang, Feng Li, Hao Zhang, Kaichen Zhang, Peiyuan Zhang, Yanwei Li, Ziwei Liu, et al. 2024. Llava-onevision: Easy visual task transfer. *arXiv preprint arXiv:2408.03326* (2024).

[20] KunChang Li, Yinan He, Yi Wang, Yizhuo Li, Wenhai Wang, Ping Luo, Yali Wang, Limin Wang, and Yu Qiao. 2025. Videochat: Chat-centric video understanding. *Science China Information Sciences* 68, 10 (2025), 200102.

[21] Kunchang Li, Yali Wang, Yinan He, Yizhuo Li, Yi Wang, Yi Liu, Zun Wang, Jilan Xu, Guo Chen, Ping Luo, et al. 2024. Mvbench: A comprehensive multi-modal video understanding benchmark. In *Proceedings of the IEEE/CVF Conference on Computer Vision and Pattern Recognition*. 22195–22206.

[22] Xiang Lisa Li and Percy Liang. 2021. Prefix-tuning: Optimizing continuous prompts for generation. In *Proceedings of the 59th Annual Meeting of the Association for Computational Linguistics and the 11th International Joint Conference on Natural Language Processing (Volume 1: Long Papers)*. 4582–4597.

[23] Yulin Li, Haokun Gui, Ziyang Fan, Junjie Wang, Bin Kang, Bin Chen, and Zhuotao Tian. 2025. Less Is More, but Where? Dynamic Token Compression via LLM-Guided Keyframe Prior. *arXiv preprint arXiv:2512.06866* (2025).

[24] Yanwei Li, Chengyao Wang, and Jiaya Jia. 2024. Llama-vid: An image is worth 2 tokens in large language models. In *European Conference on Computer Vision*. Springer, 323–340.

[25] Bin Lin, Yang Ye, Bin Zhu, Jiaxi Cui, Munan Ning, Peng Jin, and Li Yuan. 2024. Video-llava: Learning united visual representation by alignment before projection. In *Proceedings of the 2024 conference on empirical methods in natural language processing*. 5971–5984.

[26] Ruyang Liu, Chen Li, Haoran Tang, Yixiao Ge, Ying Shan, and Ge Li. 2024. St-llm: Large language models are effective temporal learners. In *European Conference on Computer Vision*. Springer, 1–18.

[27] Ruipu Luo, Ziwang Zhao, Min Yang, Zheming Yang, Minghui Qiu, Zhongyu Wei, Yanhao Wang, and Cen Chen. 2026. Valley: Video Assistant with Large Language Model Enhanced Ability. *ACM Transactions on Multimedia Computing, Communications, and Applications* 22, 7 (2026), 1–25. doi:10.1145/3796716

[28] Muhammad Maaz, Hanoona Rasheed, Salman Khan, and Fahad Khan. 2024. Video-chatgpt: Towards detailed video understanding via large vision and language models. In *Proceedings of the 62nd Annual Meeting of the Association for Computational Linguistics (Volume 1: Long Papers)*. 12585–12602.

[29] Karttikeya Mangalam, Raiymbek Akshulakov, and Jitendra Malik. 2023. Egoschema: A diagnostic benchmark for very long-form video language understanding. *Advances in Neural Information Processing Systems* 36 (2023), 46212–46244.

[30] Victor Sanh, Lysandre Debut, Julien Chaumond, and Thomas Wolf. 2019. DistilBERT, a distilled version of BERT: smaller, faster, cheaper and lighter. *arXiv preprint arXiv:1910.01108* (2019).

[31] Yuzhang Shang, Mu Cai, Bingxin Xu, Yong Jae Lee, and Yan Yan. 2025. Llava-prumerge: Adaptive token reduction for efficient large multimodal models. In *Proceedings of the IEEE/CVF International Conference on Computer Vision*. 22857–22867.

[32] Kele Shao, Keda Tao, Can Qin, Haoxuan You, Yang Sui, and Huan Wang. 2025. Holitom: Holistic token merging for fast video large language models. *arXiv preprint arXiv:2505.21334* (2025).

[33] Leqi Shen, Guoqiang Gong, Tao He, Yifeng Zhang, Pengzhang Liu, Sicheng Zhao, and Guiguang Ding. 2025. Fastvid: Dynamic density pruning for fast video large language models. *arXiv preprint arXiv:2503.11187* (2025).

[34] Enxin Song, Wenhao Chai, Guanhong Wang, Yucheng Zhang, Haoyang Zhou, Feiyang Wu, Haozhe Chi, Xun Guo, Tian Ye, Yanting Zhang, et al. 2024. Moviechat: From dense token to sparse memory for long video understanding. In *Proceedings of the IEEE/CVF Conference on Computer Vision and Pattern Recognition*. 18221–18232.

[35] Keda Tao, Can Qin, Haoxuan You, Yang Sui, and Huan Wang. 2025. Dycoke: Dynamic compression of tokens for fast video large language models. In *Proceedings of the Computer Vision and Pattern Recognition Conference*. 18992–19001.

[36] Peng Wang, Shuai Bai, Sinan Tan, Shijie Wang, Zhihao Fan, Jinze Bai, Keqin Chen, Xuejing Liu, Jialin Wang, Wenbin Ge, et al. 2024. Qwen2-vl: Enhancing vision-language model's perception of the world at any resolution. *arXiv preprint arXiv:2409.12191* (2024).

[37] Wenhui Wang, Furu Wei, Li Dong, Hangbo Bao, Nan Yang, and Ming Zhou. 2020. Minilm: Deep self-attention distillation for task-agnostic compression of pre-trained transformers. *Advances in neural information processing systems* 33 (2020), 5776–5788.

[38] Haoning Wu, Dongxu Li, Bei Chen, and Junnan Li. 2024. Longvideobench: A benchmark for long-context interleaved video-language understanding. *Advances in Neural Information Processing Systems* 37 (2024), 28828–28857.

[39] Long Xing, Qidong Huang, Xiaoyi Dong, Jiajie Lu, Pan Zhang, Yuhang Zang, Yuhang Cao, Conghui He, Jiaqi Wang, Feng Wu, et al. 2024. Pyramiddrop: Accelerating your large vision-language models via pyramid visual redundancy reduction. *arXiv preprint arXiv:2410.17247* (2024).

[40] Lin Xu, Yilin Zhao, Daquan Zhou, Zhijie Lin, See Kiong Ng, and Jiashi Feng. 2024. Pllava: Parameter-free llava extension from images to videos for video dense captioning. *arXiv preprint arXiv:2404.16994* (2024).

[41] Cheng Yang, Yang Sui, Jinqi Xiao, Lingyi Huang, Yu Gong, Chendi Li, Jinghua Yan, Yu Bai, Ponnuswamy Sadayappan, Xia Hu, et al. 2025. Topv: Compatible token pruning with inference time optimization for fast and low-memory multimodal vision language model. In *Proceedings of the Computer Vision and Pattern Recognition Conference*. 19803–19813.

[42] Senqiao Yang, Yukang Chen, Zhuotao Tian, Chengyao Wang, Jingyao Li, Bei Yu, and Jiaya Jia. 2025. Visionzip: Longer is better but not necessary in vision language models. In *Proceedings of the IEEE/CVF Conference on Computer Vision and Pattern Recognition*. 19792–19802.

[43] Ce Zhang, Kaixin Ma, Tianqing Fang, Wenhao Yu, Hongming Zhang, Zhisong Zhang, Yaqi Xie, Katia Sycara, Haitao Mi, and Dong Yu. 2025. Vscan: Rethinking visual token reduction for efficient large vision-language models. *arXiv preprint arXiv:2505.22654* (2025).

[44] Hang Zhang, Xin Li, and Lidong Bing. 2023. Video-llama: An instruction-tuned audio-visual language model for video understanding. In *Proceedings of the 2023 conference on empirical methods in natural language processing: system demonstrations*. 543–553.

[45] Jusheng Zhang, Kaitong Cai, Yijia Fan, Ningyuan Liu, and Keze Wang. 2025. MAT-Agent: Adaptive Multi-Agent Training Optimization. In *The Thirty-ninth Annual Conference on Neural Information Processing Systems*. https://openreview.net/forum?id=YDWRTYgR79

[46] Jusheng Zhang, Kaitong Cai, Yijia Fan, Jian Wang, and Keze Wang. 2025. CF-VLM: Counterfactual Vision-Language Fine-tuning. In *The Thirty-ninth Annual Conference on Neural Information Processing Systems*. https://openreview.net/forum?id=0qGtaRTsCo

[47] Jusheng Zhang, Kaitong Cai, Xiaoyang Guo, Sidi Liu, Qinhan Lv, Ruiqi Chen, Jing Yang, Yijia Fan, Xiaofei Sun, Jian Wang, Ziliang Chen, Liang Lin, and Keze Wang. 2025. MM-CoT:A Benchmark for Probing Visual Chain-of-Thought Reasoning in Multimodal Models. arXiv:2512.08228 [cs.CV] https://arxiv.org/abs/2512.08228

[48] Jusheng Zhang, Kaitong Cai, Jing Yang, Ziliang Chen, Yongsen Zheng, Kwok-Yan Lam, Liang Lin, and Keze Wang. 2026. Failure-Driven Workflow Refinement. In *Forty-third International Conference on Machine Learning*. https://openreview.net/forum?id=GbYHY1RVUa

[49] Jusheng Zhang, Kaitong Cai, Jing Yang, Jian Wang, and Keze Wang. 2026. Dynamics-Aware Preference Optimization for Vision-Language Models. In *Proceedings of the IEEE/CVF Conference on Computer Vision and Pattern Recognition (CVPR)*. 11610–11620.

[50] Jusheng Zhang, Yijia Fan, Kaitong Cai, Xiaofei Sun, and Keze Wang. 2025. OSC: Cognitive Orchestration through Dynamic Knowledge Alignment in Multi-Agent LLM Collaboration. arXiv:2509.04876 [cs.AI] https://arxiv.org/abs/2509.04876

[51] Jusheng Zhang, Yijia Fan, Kaitong Cai, Keze Wang, and Wenhao Wang. 2026. Kolmogorov-Arnold Fourier Networks. arXiv:2502.06018 [cs.LG] https://arxiv.org/abs/2502.06018

[52] Jusheng Zhang, Yijia Fan, Kaitong Cai, Jing Yang, Jiawei Yao, Jian Wang, Guanlong Qu, Ziliang Chen, and Keze Wang. 2026. Why Keep Your Doubts to Yourself? Trading Visual Uncertainties in Multi-Agent Bandit Systems. arXiv:2601.18735 [cs.AI] https://arxiv.org/abs/2601.18735

[53] Jusheng Zhang, Yijia Fan, Wenjun Lin, Ruiqi Chen, Haoyi Jiang, Wenhao Chai, Jian Wang, and Keze Wang. 2025. GAM-Agent: Game-Theoretic and Uncertainty-Aware Collaboration for Complex Visual Reasoning. In *The Thirty-ninth Annual Conference on Neural Information Processing Systems*. https://openreview.net/forum?id=EKJhU5ioSo

[54] Jusheng Zhang, Yijia Fan, Zimo Wen, Jian Wang, and Keze Wang. 2025. Tri-MARF: A Tri-Modal Multi-Agent Responsive Framework for Comprehensive 3D Object Annotation. In *The Thirty-ninth Annual Conference on Neural Information Processing Systems*. https://openreview.net/forum?id=YGIbwfNWot

[55] Jusheng Zhang, Xiaoyang Guo, Kaitong Cai, Qinhan Lv, Yijia Fan, Wenhao Chai, Jian Wang, and Keze Wang. 2025. HybridToken-VLM: Hybrid Token Compression for Vision-Language Models. arXiv:2512.08240 [cs.CV] https://arxiv.org/abs/2512.08240

[56] Jusheng Zhang, Zimeng Huang, Yijia Fan, Ningyuan Liu, Mingyan Li, Zhuojie Yang, Jiawei Yao, Jian Wang, and Keze Wang. 2025. KABB: Knowledge-Aware Bayesian Bandits for Dynamic Expert Coordination in Multi-Agent Systems. In *Forty-second International Conference on Machine Learning*. https://openreview.net/forum?id=AKvy9a4jho

[57] Jusheng Zhang, Qinhan Lyu, Sizhuo Ma, Rick Cao, Jian Wang, Xin Li, Yongsen Zheng, Keze Wang, Jing Yang, Hong Zhang, et al. 2026. The 1st LoViF Challenge on Efficient VLM for Multimodal Ad Creative Quality Scoring: Methods and Results. In *Proceedings of the IEEE/CVF Conference on Computer Vision and Pattern Recognition*. 5138–5147.

[58] Qingru Zhang, Minshuo Chen, Alexander Bukharin, Nikos Karampatziakis, Pengcheng He, Yu Cheng, Weizhu Chen, and Tuo Zhao. 2023. Adalora: Adaptive budget allocation for parameter-efficient fine-tuning. *arXiv preprint arXiv:2303.10512* (2023).

[59] Qizhe Zhang, Aosong Cheng, Ming Lu, Renrui Zhang, Zhiyong Zhuo, Jiajun Cao, Shaobo Guo, Qi She, and Shanghang Zhang. 2025. Beyond text-visual attention: Exploiting visual cues for effective token pruning in vlms. In *Proceedings of the IEEE/CVF International Conference on Computer Vision*. 20857–20867.

[60] Yuan Zhang, Chun-Kai Fan, Junpeng Ma, Wenzhao Zheng, Tao Huang, Kuan Cheng, Denis Gudovskiy, Tomoyuki Okuno, Yohei Nakata, Kurt Keutzer, et al. 2024. Sparsevlm: Visual token sparsification for efficient vision-language model inference. *arXiv preprint arXiv:2410.04417* (2024).

[61] Yuanhan Zhang, Jinming Wu, Wei Li, Bo Li, Zejun Ma, Ziwei Liu, and Chunyuan Li. 2024. Llava-video: Video instruction tuning with synthetic data. *arXiv preprint arXiv:2410.02713* (2024).

[62] Orr Zohar, Xiaohan Wang, Yonatan Bitton, Idan Szpektor, and Serena Yeung-Levy. 2024. Video-star: Self-training enables video instruction tuning with any supervision. *arXiv preprint arXiv:2407.06189* (2024).